Delta Networks for Optimized Recurrent Network Computation

Daniel Neil [1] **Jun Haeng Lee** [2] **Tobi Delbruck** [1] **Shih-Chii Liu** [1]

Abstract

Many neural networks exhibit stability in their activation patterns over time in response to inputs from sensors operating under real-world conditions. By capitalizing on this property of natural signals, we propose a Recurrent Neural Network (RNN) architecture called a delta network in which each neuron transmits its value only when the change in its activation exceeds a threshold. The execution of RNNs as delta networks is attractive because their states must be stored and fetched at every timestep, unlike in convolutional neural networks (CNNs). We show that a naive run-time delta network implementation offers modest improvements on the number of memory accesses and computes, but optimized training techniques confer higher accuracy at higher speedup. With these optimizations, we demonstrate a 9X reduction in cost with negligible loss of accuracy for the TIDIGITS audio digit recognition benchmark. Similarly, on the large Wall Street Journal (WSJ) speech recognition benchmark, pretrained networks can also be greatly accelerated as delta networks and trained delta networks show a 5.7X improvement with negligible loss of accuracy. Finally, on an end-to-end CNN-RNN network trained for steering angle prediction in a driving dataset, the RNN cost can be reduced by a substantial 100X.

1. Introduction

Recurrent Neural Networks (RNNs) have achieved tremendous progress in recent years, with the increased availability of large datasets, more powerful computer resources such as GPUs, and improvements in their training algorithms. These combined factors have enabled breakthroughs in the use of RNNs for processing of temporal sequences. Applications such as natural language processing (Mikolov et al., 2010), speech recognition (Amodei et al., 2015; Graves et al., 2013), and attention-based models for structured prediction (Yao et al., 2015; Xu et al., 2015) have showcased the advantages of RNNs. The introduction of gating units such as long short-term memory (LSTM) units (Hochreiter & Schmidhuber, 1997) and gated recurrent units (GRU) (Cho et al., 2014) has greatly improved the training process with these networks. However, RNNs require many matrix-vector multiplications per layer to calculate the updates of neuron activations over time.

RNNs also require a large weight memory storage that is expensive to allocate to on-chip static random access memory (SRAM). In a 45nm technology, the energy cost of an off-chip 32-bit dynamic DRAM access is about 2nJ and the energy for a 32-bit integer multiply is about 3pJ, so memory access is about 700 times more expensive than arithmetic (Horowitz, 2014). Architectures can benefit from minimizing the use of this external memory. Previous work focused on a variety of algorithmic optimizations for reducing compute and memory access requirements for deep neural networks. These methods include reduced precision for hardware optimization (Courbariaux et al., 2015; Stromatias et al., 2015; Courbariaux & Bengio, 2016; Esser et al., 2016; Rastegari et al., 2016); weight encoding, pruning, and compression (Han et al., 2015; 2016); and architectural optimizations (Iandola et al., 2016; Szegedy et al., 2015; Huang et al., 2016). However these studies did not consider the temporal properties of the data.

Natural inputs to a neural network tend to have a high degree of temporal autocorrelation, resulting in slowly-changing network states. This slow-changing activation feature is also seen within the computation of RNNs processing audio inputs, for example, speech (Fig. 1).

Delta networks, as introduced here, exploit the temporal stability of both the input stream and the associated neural representation to reduce memory access and computation without loss of accuracy. By caching neuron activations, computations can be skipped where inputs change by a small amount from the previous update. Because each neuron that is not updated will save fetches of entire columns of several weight matrices, determining which

[1]Institute of Neuroinformatics, UZH and ETH Zurich, Zurich, Switzerland [2]Samsung Advanced Institute of Technology, Samsung Electronics, Suwon-Si, Republic of Korea. Correspondence to: Daniel Neil, Shih-Chii Liu <dneil,shih@ini.ethz.ch>.

Proceedings of the 34th International Conference on Machine Learning, Sydney, Australia, PMLR 70, 2017. Copyright 2017 by the author(s).

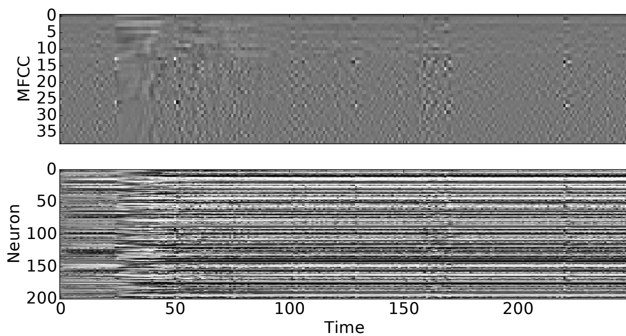

Figure 1. Stability in RNN activations over time. The top figure shows the continually-changing MFCC features for a spoken digit from the TIDIGITS dataset (Leonard & Doddington, 1993); the bottom figure shows the corresponding neural network output activations in response to these features. Note the slow evolution of the network states over timesteps.

neurons need to be updated offers significant speedups.

The rest of the paper is organized as follows. Sec. 2 introduces the delta network concept in terms of the basic matrix-vector operations. Sec. 3 formulates it concretely for a GRU RNN. Sec. 4 proposes a method using a finite threshold for the deltas that suppresses the accumulation of the transient approximation error. Sec. 5 describes methods for optimally training a delta RNN. Sec. 6 shows network accuracy versus speedup for three examples. Finally, Sec. 7 summarizes the results.

2. Delta Network Formulation

The purpose of a delta network is to transform a dense matrix-vector multiplication (for example, a weight matrix and a state vector) into a sparse matrix-vector multiplication followed by a full addition. This transformation leads to savings on both operations (actual multiplications) and more importantly memory accesses (weight fetches). Fig. 2 illustrates the savings due to a sparse multiplicative vector. Zeros are shown with white, while non-zero matrix and vector values are shown in black. Note the multiplicative effect of sparsity in the weight matrix and sparsity in the delta vector. In this example, 20% occupancy of the weight matrix and 20% occupancy of the Δ vector requires fetching and computing only 4% of the original operations.

To illustrate the delta network methodology, consider a general matrix-vector multiplication of the form

$$r = Wx \tag{1}$$

that uses n^2 compute operations[1], n^2+n reads and n writes for a W matrix of size $n \times n$ and a vector x of size n.

[1] In this paper, a "compute" operation is either a multiply, an add, or a multiply-accumulate. The costs of these operations are similar, particularly when compared to the cost of an off-chip memory operation. See (Horowitz, 2014) for a simple comparison of energy costs of compute and memory operations.

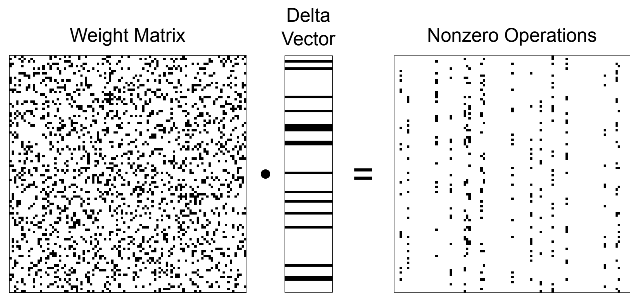

Figure 2. Illustration of saved matrix-vector computation using delta networks with sparse delta vectors and weight matrices.

Now consider multiple matrix-vector multiplications for a long input vector sequence x_t indexed by $t = 1, 2, \ldots$. The result r_t can be calculated recursively as:

$$r_t = W\Delta + r_{t-1}, \tag{2}$$

where $\Delta = x_t - x_{t-1}$ and r_{t-1} is the result obtained from the previous calculation; if stored, the compute cost of r_{t-1} is zero as it can be fetched from the previous timestep. Trivially, $x_0 = 0$ and $r_0 = 0$. It is clear that

$$\begin{aligned} r_t &= W(x_t - x_{t-1}) + r_{t-1} && (3)\\ &= W(x_t - x_{t-1}) + W(x_{t-1} - x_{t-2}) + \ldots + r_0 && (4)\\ &= Wx_t && (5) \end{aligned}$$

Thus this formulation, which uses the difference between two subsequent timesteps and referred to as the *delta network* formulation, can be seen to produce exactly the same result as the original matrix-vector multiplication.

2.1. Theoretical Cost Calculation

To illustrate the savings if Δ from (2) is sparse, we begin by defining o_c to be the *occupancy* of a vector , that is, the percentage of nonzero elements in the vector.

Consider the compute cost for r_t; it consists of the total cost for calculating Δ (n operations for a vector of size n), adding in the stored previous result r_{t-1} (n operations), and performing the sparse matrix multiply $W\Delta$ ($o_c \cdot n^2$ operations for a W of size $n \times n$ and a sparse Δ vector of occupancy ratio o_c). Similarly, the memory cost for calculating r_t requires fetching $o_c \cdot n^2$ weights for W, $2n$ values for Δ, n values for r_{t-1} and writing out the n values for r_t.

Overall, the compute cost for the standard formulation ($C_{\text{comp,dense}}$) and the new delta formulation ($C_{\text{comp,sparse}}$)

will be:

$$C_{\text{comp,dense}} = n^2 \quad (6)$$

$$C_{\text{comp,sparse}} = o_c \cdot n^2 + 2n \quad (7)$$

while the memory access costs for both the standard ($C_{\text{mem,dense}}$) and delta networks ($C_{\text{mem,sparse}}$) can be seen from inspection as:

$$C_{\text{mem,dense}} = n^2 + n \quad (8)$$

$$C_{\text{mem,sparse}} = o_c \cdot n^2 + 4n \quad (9)$$

Thus, the arithmetic intensity (ratio of arithmetic to memory access costs) as $n \to \infty$ is 1 for both the standard and delta network methods. This means that every arithmetic operation requires a memory access, unfortunately placing computational accelerators at a disadvantage. However, if a sparse occupancy o_c of Δ is assumed, then the decrease in computes and memory accesses due to storing the previous state will result in a speedup of:

$$C_{\text{dense}}/C_{\text{sparse}} \approx n^2/(o_c \cdot n^2) = (1/o_c) \quad (10)$$

For example, if $o_c = 10\%$, then the theoretical speedup will be 10X. Note that this speedup is determined by the occupancy in each computed $\Delta = x_t - x_{t-1}$, implying that this sparsity is determined by the data stream. Specifically, the regularity with which values stay exactly the same between x_t and x_{t-1}, or as demonstrated later, within a certain absolute value called the threshold, determines the speedup. In a neural network, x can represent inputs, intermediate activation values, or outputs of the network. If x changes slowly between subsequent timesteps then the input values x_t and x_{t-1} will be highly redundant, leading to a low occupancy o_c and a correspondingly increased speedup.

3. Delta Network GRUs

In GRUs, the matrix-vector multiplication operation that can be replaced with a delta network operation appears several times, shown in bold below. This GRU formulation is from (Chung et al., 2014):

$$r_t = \sigma_r(\mathbf{W_{xr}x_t} + \mathbf{W_{hr}h_{t-1}} + b_r) \quad (11)$$

$$u_t = \sigma_u(\mathbf{W_{xu}x_t} + \mathbf{W_{hu}h_{t-1}} + b_u) \quad (12)$$

$$c_t = \sigma_c(\mathbf{W_{xc}x_t} + r_t \odot (\mathbf{W_{hc}}h_{t-1}) + b_c) \quad (13)$$

$$h_t = (1 - u_t) \odot h_{t-1} + u_t \odot c_t \quad (14)$$

Here r, u, c and h are reset and update gates, candidate activation, and activation vectors, respectively, typically a few hundred elements long. The σ functions are nonlinear logistic sigmoids that saturate at 0 and 1. The $\odot$ signifies element-wise multiplication. Each term in bold can be replaced with the delta update defined in (2), forming:

$$\Delta_x = x_t - x_{t-1} \quad (15)$$

$$\Delta_h = h_{t-1} - h_{t-2} \quad (16)$$

$$r_t = \sigma_r(W_{xr}\Delta_x + z_{xr} + W_{hr}\Delta_h + z_{hr} + b_r) \quad (17)$$

$$u_t = \sigma_u(W_{xu}\Delta_x + z_{xu} + W_{hu}\Delta_h + z_{hu} + b_u) \quad (18)$$

$$c_t = \sigma_c(W_{xc}\Delta_x + z_{xc} + b_c \\ r_t \odot (W_{hc}\Delta_h + z_{hc})) \quad (19)$$

$$h_t = (1 - u_t) \odot h_{t-1} + u_t \odot c_t \quad (20)$$

where the values z_{xr}, z_{xu}, z_{xc}, z_{hr}, z_{hu}, z_{hc} are recursively defined as the the stored result of the previous computation for the input or hidden state, i.e.:

$$z_{xr} := \quad z_{xr,t-1} = \quad W_{xr}(x_{t-1} - x_{t-2}) + z_{xr,t-2} \quad (21)$$

The above operation can be applied for the other five values z_{xu}, z_{xc}, z_{hr}, z_{hu}, z_{hc}. The initial condition at time x_0 is $z_0 := 0$. Also, many of the additive terms in the equations above, including the stored full-rank pre-activation states as well as the biases, can be merged into single values resulting into four stored memory values (M_r, M_u, M_{xc}, and M_{hr}) for the three gates:

$$M_{t-1} := z_{x,t-1} + z_{h,t-1} + b \quad (22)$$

Finally, in accordance with the above definitions of the initial state, the memories M are initialized at their corresponding biases, i.e., $M_{r,0} = b_r$, $M_{u,0} = b_u$, $M_{xc,0} = b_c$, and $M_{hr,0} = 0$, resulting in the following full formulation of the delta network GRU:

$$\Delta_x = x_t - x_{t-1} \quad (23)$$

$$\Delta_h = h_{t-1} - h_{t-2} \quad (24)$$

$$M_{r,t} := W_{xr}\Delta_x + W_{hr}\Delta_h + M_{r,t-1} \quad (25)$$

$$M_{u,t} := W_{xu}\Delta_x + W_{hu}\Delta_h + M_{u,t-1} \quad (26)$$

$$M_{xc,t} := W_{xc}\Delta_x + M_{xc,t-1} \quad (27)$$

$$M_{hc,t} := W_{hc}\Delta_h + M_{hc,t-1} \quad (28)$$

$$r_t = \sigma_r(M_{r,t}) \quad (29)$$

$$u_t = \sigma_u(M_{u,t}) \quad (30)$$

$$c_t = \sigma_c(M_{xc,t} + r_t \odot M_{hc,t}) \quad (31)$$

$$h_t = (1 - u_t) \odot h_{t-1} + u_t \odot c_t \quad (32)$$

4. Delta Network Approximations

The formulations described in Secs. 2 and 3 are designed to give precisely the same answer as the original computation in the network. However, a more aggressive approach can be taken in the update, inspired by recent studies that have shown the possibility of greatly reducing weight precision in neural networks without giving up accuracy (Stromatias et al., 2015; Courbariaux et al., 2014). Instead of skipping

a vector-multiplication computation if a change in the activation $\Delta = 0$, a vector-multiplication can be skipped if a value of Δ is smaller than the threshold (i.e $|\Delta_{i,t}| < \Theta$, where Θ is a chosen threshold value for a state i at time t). That is, if a neuron's hidden-state M activation has changed by less than Θ since it was last memorized, the neuron output will not be propagated, i.e., its Δ value is set to zero for that update. Using this threshold, the network will not produce precisely the same result at each update, but will produce a result which is approximately correct. Moreover, the use of a threshold substantially increases activation sparsity.

Importantly, if a non-zero threshold is used with a naive delta change propagation, errors can accumulate over multiple time steps through state drift. For example, if the input value x_t increases by nearly Θ on every time step, no change will ever be triggered despite an accumulated significant change in activation, causing a large drift in error. Therefore, in our implementation, the memory records the last value causing an above-threshold change, not the difference since the last time step.

More formally, we introduce the states $\hat{x}_{i,t-1}$ and $\hat{h}_{j,t-1}$. These states store the $i-$th input and the hidden state of the $j-$th neurons, respectively, at their last *change*. The current input $x_{i,t}$ and state $h_{j,t}$ will be compared against these values to determine the Δ. Then the $\hat{x}_{i,t-1}$ and $\hat{h}_{j,t-1}$ values will only be updated if the threshold Θ is crossed. The equations are shown below for $\hat{x}_{i,t-1}$ with similar equations for $\hat{h}_{j,t-1}$:

$$\hat{x}_{i,t-1} = \begin{cases} x_{i,t-1} & \text{if } |x_{i,t} - \hat{x}_{i,t-1}| > \Theta \\ \hat{x}_{i,t-2} & \text{otherwise} \end{cases} \tag{33}$$

$$\Delta x_{i,t} = \begin{cases} x_{i,t} - \hat{x}_{i,t-1} & \text{if } |x_{i,t} - \hat{x}_{i,t-1}| > \Theta \\ 0 & \text{otherwise} \end{cases} \tag{34}$$

That is, when calculating the input delta vector $\Delta x_{i,t}$ comprised of each element i at time t, the difference between two values are used: the current value of the input $x_{i,t}$, and the value the last time the delta vector was nonzero $\hat{x}_{i,t-1}$. Furthermore, if the delta change is less than Θ, then the delta change is set to zero, producing a small approximation error that will be corrected when a sufficiently large change produces a nonzero update. The same formulation is used for the hidden state delta vector $\Delta h_{j,t}$.

This input approximation does not guarantee that the output error is bounded by the same threshold Θ. As supported by previous studies demonstrating that GRUs can be arbitrarily sensitive to input perturbations (Laurent & von Brecht, 2016), the per-timestep error can grow with the input error. While thresholding should offer greater sparsity, the accumulation of these approximations could result in a diverging output error, therefore motivating the experiments in Sec. 6.1 that examine the effect of approximation on trajectory evolution.

5. Methods to Increase Accuracy & Speedup

This section presents training methods and optimization schemes for faster and more accurate delta networks.

5.1. Training Directly on Delta Networks

The most principled method of training to minimize accuracy loss when running as a delta network would be to train directly on the delta network model. This should yield the best results as the network will receive errors that arise directly from the truncations of the delta network computation, and through training, learn to become robust to the types of errors that delta networks make.

More accurately, instead of training on the original GRU equations Eq. 11–14, the state is updated using the delta network model described in Eq. 23–34. Importantly, this change should incur no accuracy loss between train accuracy and test accuracy, though gradient descent may yet have more difficulty optimizing the model during training.

5.2. Rounding Network Activations

As the truncation of network activation due to the delta network is inherently non-differentiable, this training method should be compared against more widely used methods to verify its effectiveness. The delta network's computation can be viewed as analogous to the reduced-precision rounding training methods; small changes are rounded to zero while larger changes are propagated. Since many previous investigations have demonstrated methods to train networks to be robust against small rounding errors by rounding during training (Courbariaux et al., 2014; Stromatias et al., 2015), these methods can be leveraged here to train a network that does not rely on small fluctuations in inputs. Low-precision computation and parameters can further reduce power consumption and improve the efficiency of the network for dedicated hardware implementations.

As in other studies, a low-resolution activation θ_L in signed fixed-point format $Qm.f$ with m integer bits and f fractional bits can be produced from a high-resolution activation θ by using a deterministic and gradient-preserving rounding: $\theta_L = \text{round}(2^f \cdot \theta) \cdot 2^{-f}$ with $2^f \cdot \theta$ clipped to a bounding range $[-2^{m+f-1}, 2^{m+f-1}]$ to produce a quantized fixed-point activation. The output error cost forces the network to avoid quantization errors during training.

5.3. Adding Gaussian Noise to Network Activations

Random noise injection provides another useful comparison point. By injecting noise, the network will be un-

able to rely on small changes, and occasionally even larger changes will be incorrect (as may be the case of threshold rounding). This robustness can be provided by adding Gaussian noise η to terms that will have a thresholded delta activation:

$$r_t = \sigma_r((x_t + \eta_x)W_{xr} + (h_{t-1} + \eta_h)W_{hr} + b_r) \quad (35)$$

$$u_t = \sigma_u((x_t + \eta_x)W_{xu} + (h_{t-1} + \eta_h)W_{hu} + b_u) \quad (36)$$

$$c_t = \sigma_c((x_t + \eta_x)W_{xc} + r_t \odot ((h_{t-1} + \eta_h)W_{hc}) + b_c) \quad (37)$$

$$h_t = (1 - u_t) \odot h_{t-1} + u_t \odot c_t \quad (38)$$

where $\eta \sim \mathcal{N}(\mu, \sigma)$. That is, η is a vector of samples drawn from the Gaussian distribution with mean μ and variance σ, and $\eta \in \{\eta_x, \eta_h\}$. Each element of these vectors is drawn independently. Typically, the value μ is set to 0 so that the expectation is unbiased, e.g., $\mathbf{E}[x_t + \eta_x] = \mathbf{E}[x_t]$.

As a result, the Gaussian noise should prevent the network from being sensitive to minor fluctuations, and increase its robustness to truncation errors.

5.4. Considering Weight Sparsity

In all training methods, considering the additional speedup from weight sparsity, in addition to skipping activation computation, should improve the theoretical speedup. Studies such as in (Ott et al., 2016) show that in trained low-precision networks, the weight matrices can be quite sparse. For example, in a ternary or 3-bit weight network the weight matrix sparsity can exceed 80% for small RNNs. Since every nonzero input vector element is multiplied by a column of the weight matrix, this computation can be skipped if the weight value is zero. That is, the zeros in the weight matrix act multiplicatively with the delta vector to produce even fewer necessary multiply-accumulates, as illustrated above in Fig. 2. The compute cost of the matrix-vector product will be $C_{\text{comp,sparse}} = o_m \cdot o_c \cdot n^2 + 2n$ and the memory cost will be $C_{\text{mem,sparse}} = o_m \cdot o_c \cdot n^2 + 4n$ for a weight matrix with occupancy o_m. By comparison to Eq. 10, the system can achieve a theoretical speedup of $1/(o_m \cdot o_c)$. That is, by compressing the weight matrix and only fetching nonzero weight elements that combine with the nonzero state vector, a higher speedup can be obtained without degrading the accuracy.

5.5. Incurring Sparsity Cost on Changes in Activation

Finally, a computation-specific cost can be associated with the delta terms and added to the overall cost. In an input batch, the L_1 norm for Δ_h can be calculated as the mean absolute delta changes, and this norm can be scaled by a weighting factor β. This L_{sparse} cost ($\mathcal{L}_{\text{sparse}} = \beta||\Delta h||_1$) can then be additively incorporated into the standard loss function. Here the L_1 norm is used to encourage sparse values in Δh, so that fewer delta updates are required.

6. Results

This section presents results demonstrating the trade-off between compute savings and accuracy loss, using Delta Network RNNs trained on the TIDIGITS digit recognition benchmark. Furthermore, it also demonstrates that the results found on small datasets also translate to the much larger Wall Street Journal speech recognition benchmark. The final example is for a CNN-RNN stack trained on end-to-end steering prediction using a recent driving dataset. The fixed-point $Q3.4$ (i.e. $m = 3$ and $f = 4$) format was used for network activation values in all speech experiments except the "Original" RNN line for TIDIGITS in Fig. 4, which was trained in floating-point representation. The driving dataset in Sec. 6.4 used $Q2.5$ activation. The networks were trained with Lasagne (Dieleman et al., 2015) powered by Theano (Bergstra et al., 2010). Reported training time is for a single Nvidia GTX 980 Ti GPU.

6.1. TIDIGITS Dataset Trajectory Evolution

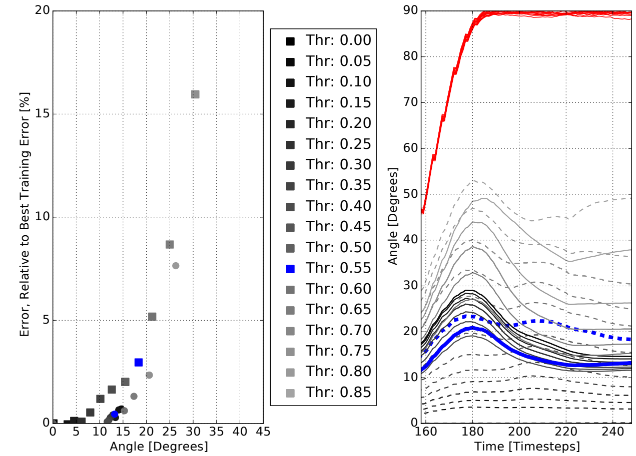

Figure 3. Comparison of trajectories over time by increasing Θ from 0 to 0.85 in steps of 0.05. At left, an increase of error angle between the final training state and the final thresholded state manifests as a decrease in accuracy, with the Gaussian-trained net as squares and DN-trained net as circles. At right, the mean angle between the unapproximated state and the thresholded state over time. In red, the angle over time of an untrained network that has the same weight statistics as a trained network; in solid lines, a network that was trained as a delta network; in dashed lines, a network that was only trained with Gaussian noise. Curves for $\Theta = 0.55$ are highlighted in blue. Note that a DN-trained network has lower angle error, especially at higher thresholds, and an untrained net always quickly converges to an orthogonal state.

The TIDIGITS dataset was used as an initial evaluation task to study the trajectory evolution of delta networks. Single digits ("oh" and zero through nine), totalling 2464 dig-

its in the training set and 2486 digits in the test set, were transformed in the standard way (Neil & Liu, 2016) to produce a 39-dimensional Mel-Frequency Cepstral Coefficient (MFCC) feature vector using a 25 ms window, 10 ms frame shift, and 20 filter bank channels. The labels for “oh” and “zero” were collapsed to a single label. Training time is approximately 8 minutes for a 150 epoch experiment.

The network architecture consists of a layer of 200 GRU units connected to a layer of 200 fully-connected units and finally to a classification layer for the 10 digit classes. First, a network was trained with Gaussian noise injection (Sec. 5.3) and subsequently tested using the delta network GRU formulation given in Sec. 3. A second network was trained directly on the delta network GRU formulation in accordance with Sec. 5.1, with the same architecture and $\Theta = 0.5$. Finally, a third network was constructed from the DN-trained network by permuting its weights to produce an “untrained” network with identical weight statistics.

To determine the robustness of the network to thresholded input, the trajectory evolution of these three networks were examined in comparison to their training conditions. Since the hidden states are bounded by (-1, 1) from the tanh nonlinearity, each 200-dimensional hidden state vector is normalized to construct a unit vector. Then, the error angle between the hidden state at training time and the hidden state with a threshold is measured. This error angle is correlated with the final accuracy, as seen in Fig. 3 left. The threshold is swept from 0 to 0.85, producing the results found in Fig. 3 right, in which each line represents the mean difference angle over all states across time. The figure begins at the median start point of a digit presentation (t=158), as the digits are pre-padded with zeros to match lengths.

A Gaussian-trained network’s trajectory initially matches its training trajectory to produce a low error angle at low thresholds, which gradually increases as the threshold is raised. However, across a wide range of Θ, a DN-trained net’s trajectory matches its training trajectory much more closely to produce a tighter-spaced arrangement and substantially lower angle error at higher threshold. Finally, an untrained network is indeed very sensitive to input approximations and quickly reaches an orthogonal representation, thus emphasizing the role of training to provide robustness.

6.2. TIDIGITS Dataset Speedup and Accuracy

The results of applying the methods introduced in Sec. 5 can be found in Fig. 4. There are two quantities measured: the change in the number of memory fetches, and the accuracy as a function of the threshold Θ. Fig. 5 shows the same results, but removes the threshold axis to directly compare the accuracy-speedup tradeoff among the different training methods. First, a standard GRU RNN achieving 96.59% accuracy on TIDIGITS was trained without data augmentation and regularization. This network has the architecture described in Sec. 6.1. It was then subsequently tested using the delta network GRU formulation given in Sec. 3.

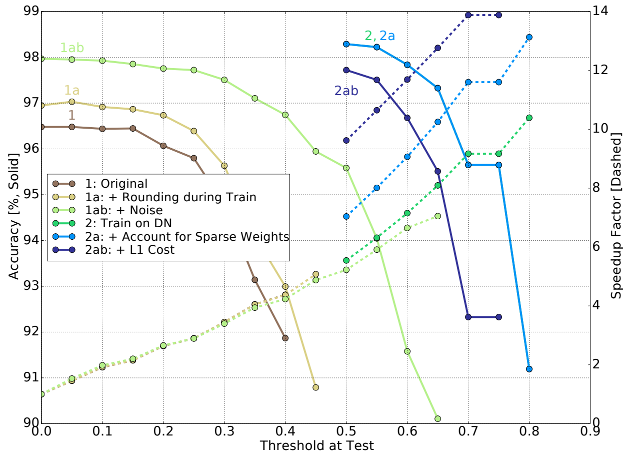

Figure 4. Test accuracy results from standard GRUs run as delta networks after training (curves **1**, **1a**, and **1ab**) and those trained as delta networks (curves **2**, **2a**, and **2ab**) under different constraints on the TIDIGITS dataset. The delta networks are trained for $\Theta = 0.5$, and the average of five runs is shown. Note that the methods are combined, hence the naming scheme. Additionally, the accuracy curve for **2** is hidden by the curve **2a**, since both achieve the same accuracy and only differ in speedup metric.

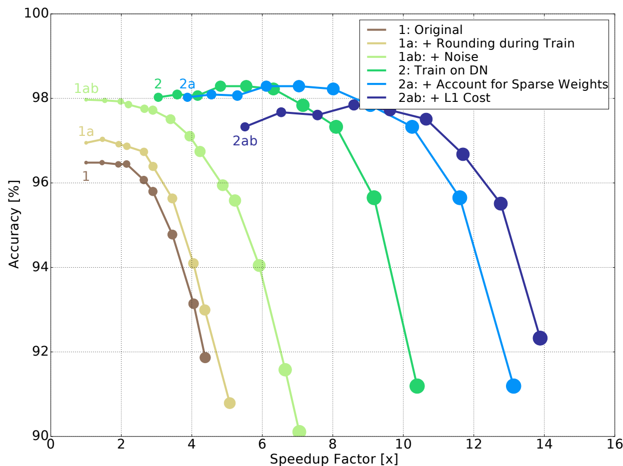

Figure 5. Accuracy-speedup tradeoff by adjusting Θ for TIDIGITS. By increasing Θ (indicated by sample point size), larger speedups can be obtained at greater losses of accuracy. For networks trained as delta networks, the training threshold is the first (leftmost) point in the line point sequence.

The standard RNN run as a delta network (“Original”) achieves 95% accuracy (a drop from zero delta threshold accuracy of 96%) with a speedup factor of about 2.2X. That is, only approximately 45% of the computes or fetches are needed in achieving this accuracy. By adding the round-

ing constraint during training ("+ Rounding during Training"), the accuracy is nearly 97% with an increase to a 3X speedup. By incorporating Gaussian noise ("+ Noise"), 97% accuracy can be maintained with a 5X speedup. Essentially, these methods added generalization robustness to the original GRU, while preventing small changes from influencing the network output. These techniques allow a higher threshold to be used while maintaining the same accuracy, therefore resulting in a decrease of memory fetches and a corresponding speedup.

The best model for training is the delta network itself ("Train on DN"). This network achieved 97.5% accuracy with a 8X speedup. Accounting for the pre-existing sparsity in the weight matrix ("+ Account for Sparse Weights"), the speedup increases to 10.5X, without affecting the accuracy (since it is the same network). Finally, incorporating an L1 cost on network changes in addition to training on the delta network model ("+ L1 cost") achieves 97% accuracy while boosting speedup to 11.9X. Adding in the final sparseness cost on network changes decreases the accuracy slightly since the loss minimization must find a tradeoff between both error and delta activation instead of considering error alone. However, using the L1 loss can offer a significant additional speedup while retaining an accuracy increase over the original GRU network.

Finally, Fig. 5 also demonstrates the primary advantage given by each algorithm; an increase in generalization robustness manifests as an overall upward shift in accuracy, while an increase in sparsity manifests as a rightward shift in speedup. As proposed, methods 1a and 1b increase generalization robustness while only modestly influencing the sparsity. Method 2 greatly increases both, while method 2a only increases sparsity, and finally method 2ab slightly decreases accuracy but offers the highest speedup.

6.3. Wall Street Journal Dataset

The delta network methodology was applied to an RNN trained on the larger WSJ dataset to determine whether it could produce the same gains as seen with the TIDIGITS dataset. This dataset comprised 81 hours of transcribed speech, as described in (Braun et al., 2016). Similar to that study, the first 4 layers of the network consisted of bidirectional GRU units with 320 units in each direction. Training time for each experiment was about 120h.

Fig. 6 presents results on the achieved word error rate (WER) and speedup on this dataset for two cases: First, running an existing speech transcription RNN as a delta network (results shown as solid curves labeled "RNN used as a DN"), and second, a network trained as a delta network with results shown as the dashed curves "Trained Delta Network". The speedup here accounts for weight matrix sparsity as described in Sec. 5.4 .

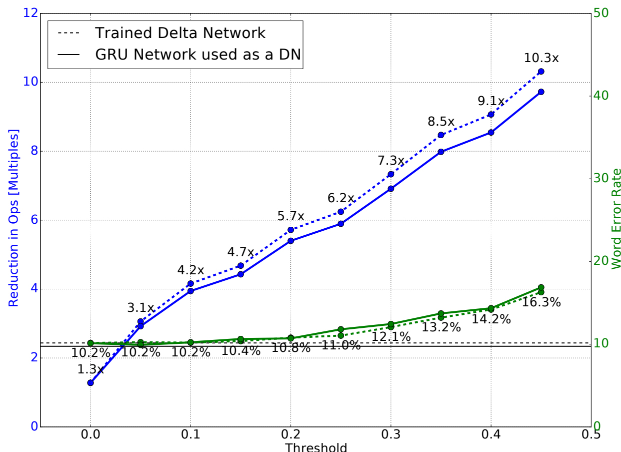

Figure 6. Accuracy and speedup tradeoffs on the WSJ dataset. The solid lines show results from an existing deep RNN run as a delta network. The dashed lines show results from a network trained as a delta network with $\Theta = 0.2$. The horizontal lines indicate the non-delta network accuracy level; similarly, the solid and dashed horizontal lines indicate the accuracy of the normal network and the DN network prior to rounding, respectively.

Surprisingly, the existing highly trained network already shows significant speedup without loss of accuracy as the threshold, Θ, is increased: At $\Theta = 0.2$, the speedup is about 5.5X with a WER of 10.8% compared with the WER of 10.2% at $\Theta = 0$. However, training the RNN to run as a delta network yields a network that achieves a slightly higher 5.7X speedup with the same WER. Thus, even the conventionally-trained RNN run as a delta network can provide greater than 5X speedup with only a 1.05X increase in the WER.

6.4. Comma.ai Driving DataSet

Driving scenarios are rapidly emerging as another area of RNN focused research. Here, the delta network model was applied to determine the gains of exploiting the redundancy of real-time video input. The open driving dataset from comma.ai (Santana & Hotz, 2016) with 7.25 hours of driving data was used, with video data recorded at 20 FPS from a camera mounted on the windshield. The network is trained to predict the steering angle from the visual scene similar to (Hempel, 2016; Bojarski et al., 2016). We followed the approach in (Hempel, 2016) by using an RNN on top of the CNN feature detector. The CNN feature detector has three convolution layers without pooling layers and a fully-connected layer with 512 units. During training, the CNN feature detector was pre-trained with an analog output unit to learn the recorded steering angle from randomly selected single frame images. Afterwards, the delta network RNN was added, and trained by feeding sequences of the visual features from the CNN feature detector to learn

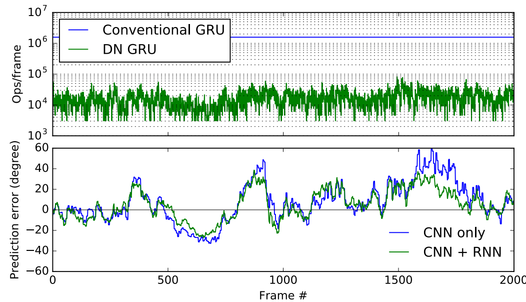

Figure 7. Reduction of RNN compute cost in the steering angle prediction task. Top figure shows the required # of ops per frame for the delta network GRU layer (trained with $\Theta = 0.1$) in comparison with the conventional GRU case. Bottom figure compares the prediction errors of CNN predictor and CNN+RNN predictor. The RNN slightly improves the steering angle prediction.

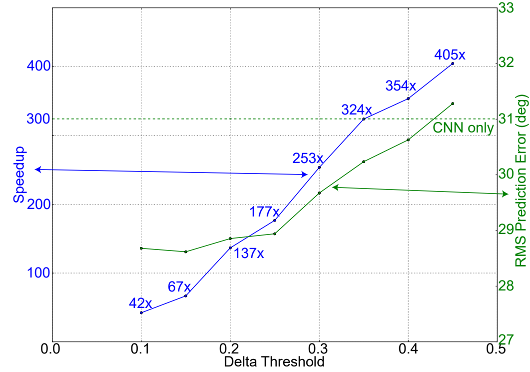

Figure 8. Tradeoffs between prediction error and speedup of the GRU layer on the steering angle prediction. The result was obtained from 1000 samples with 48 consecutive frames sampled from the validation set. Speedup here does not include weight matrix sparsity. The network was trained with $\Theta = 0.1$. A speedup of approximately 100X can be obtained without increasing the prediction error, using Θ between 0.1 and 0.25.

sequences of the steering angle. Since the Q2.5 format was used for the GRU layer activations, the GRU input vectors were scaled to match the CNN output and the target output was scaled to match the RNN output.

However, this raw dataset results in a few practical difficulties and requires data preprocessing. By excluding the frames recorded during periods of low speed driving, we remove the segments where the steering angle is not correlated to the direction of the car movement. Training time of the CNN feature detector was about 8h for 10k updates with the batch size of 200. Training of the RNN part took about 3h for 5k updates with the batch size of 32 samples consisting of 48 frames/sample.

A very large speedup exceeding 100X in the delta network GRU can be seen in Fig. 7, computed for the steering angle prediction task on 2000 consecutive frames (100s) from the validation set. While the number of operations per frame remains constant for the conventional GRU layer, those for the delta network GRU layer varies dynamically depending on the change of visual features.

In this steering network, the computational cost of the CNN (about 37 MOp/frame) dominates the RNN cost (about 1.58 MOp/frame), therefore the overall system-level computational savings is only about 4.2%. However, future applications will likely have efficient dedicated vision hardware or require a greater role for RNNs in processing numerous and complex data streams, which result in RNN models that consume a greater percentage of the overall energy/compute cost. Even now, the steering angle prediction network already benefits from a delta network approach.

7. Discussion and Conclusion

Although the delta network methodology can be applied to other network architectures, as was shown in similar concurrent work for CNNs (O'Connor & Welling, 2016), in practice a larger benefit is seen in RNNs because all the intermediate activation values for the delta networks are already stored between subsequent inputs. For example, the widely-used VGG19 CNN has 16M neuron states (Chatfield et al., 2014). Employing the delta network approach for CNNs requires doubled memory access and significant additional memory space to store the entirety of the network state. Because the cost of external memory access is hundreds of times larger than that of arithmetic operations, delta network CNNs seem impractical without novel memory technologies to address this issue.

In contrast, RNNs have a much larger number of weight parameters than activations. The sparsity of the delta activations can therefore enable large savings in power consumption by reducing the number of memory accesses required to fetch weight parameters. CNNs, however, do not have this advantage since the weight parameters are few and shared by many units. Finally, the delta network approach is extremely flexible as pre-existing networks can be used without retraining, or trained specifically for increased optimization.

Recurrent neural networks can be highly optimized due to the redundancy of their activations over time. When the use of this temporal redundancy is combined with robust training algorithms, this work demonstrates that speedups of 6X to 9X can be obtained with negligible accuracy loss in speech RNNs, and speedups of over 100X are possible in steering angle prediction RNNs, suggesting significant speedups are achievable on practical, real-world problems.

Acknowledgements

We thank S. Braun for helping with the WSJ speech transcription pipeline. This work was funded by Samsung Institute of Advanced Technology, the University of Zurich and ETH Zurich.

References

Amodei, Dario, Anubhai, Rishita, Battenberg, Eric, Case, Carl, Casper, Jared, Catanzaro, Bryan, Chen, Jingdong, Chrzanowski, Mike, Coates, Adam, Diamos, Greg, et al. Deep speech 2: End-to-end speech recognition in english and mandarin. *arXiv preprint arXiv:1512.02595*, 2015.

Bergstra, James, Breuleux, Olivier, Bastien, Frédéric, Lamblin, Pascal, Pascanu, Razvan, Desjardins, Guillaume, Turian, Joseph, Warde-Farley, David, and Bengio, Yoshua. Theano: a CPU and GPU math expression compiler. In *Proceedings of the Python for scientific computing conference (SciPy)*, volume 4, pp. 3, 2010.

Bojarski, Mariusz, Testa, Davide Del, Dworakowski, Daniel, Firner, Bernhard, Flepp, Beat, Goyal, Prasoon, Jackel, Lawrence D., Monfort, Mathew, Muller, Urs, Zhang, Jiakai, Zhang, Xin, Zhao, Jake, and Ziebam, Karol. End to end learning for self-driving cars. *arXiv preprint arXiv:1604.07316*, 2016.

Braun, Stefan, Neil, Daniel, and Liu, Shih-Chii. A curriculum learning method for improved noise robustness in automatic speech recognition. *arXiv preprint arXiv:1606.06864*, 2016.

Chatfield, Ken, Simonyan, Karen, Vedaldi, Andrea, and Zisserman, Andrew. Return of the devil in the details: Delving deep into convolutional nets. *arXiv preprint arXiv:1405.3531*, 2014.

Cho, Kyunghyun, van Merrienboer, Bart, Gulcehre, Caglar, Bougares, Fethi, Schwenk, Holger, and Bengio, Yoshua. Learning phrase representations using RNN encoder-decoder for statistical machine translation. *arXiv preprint arXiv:1406.1078*, 2014.

Chung, Junyoung, Gulcehre, Caglar, Cho, KyungHyun, and Bengio, Yoshua. Empirical evaluation of gated recurrent neural networks on sequence modeling. *arXiv preprint arXiv:1412.3555*, 2014.

Courbariaux, Matthieu and Bengio, Yoshua. Binarynet: Training deep neural networks with weights and activations constrained to+ 1 or-1. *arXiv preprint arXiv:1602.02830*, 2016.

Courbariaux, Matthieu, Bengio, Yoshua, and David, Jean-Pierre. Low precision arithmetic for deep learning. *arXiv preprint arXiv:1412.7024*, 2014.

Courbariaux, Matthieu, Bengio, Yoshua, and David, Jean-Pierre. Binaryconnect: Training deep neural networks with binary weights during propagations. In *Advances in Neural Information Processing Systems*, pp. 3123–3131, 2015.

Dieleman, Sander et al. Lasagne: First release., August 2015. URL http://dx.doi.org/10.5281/zenodo.27878.

Esser, Steven K, Merolla, Paul A, Arthur, John V, Cassidy, Andrew S, Appuswamy, Rathinakumar, Andreopoulos, Alexander, Berg, David J, McKinstry, Jeffrey L, Melano, Timothy, Barch, Davis R, et al. Convolutional networks for fast, energy-efficient neuromorphic computing. *arXiv preprint arXiv:1603.08270*, 2016.

Graves, Alan, Mohamed, Abdel-rahman, and Hinton, Geoffrey. Speech recognition with deep recurrent neural networks. In *Acoustics, Speech and Signal Processing (ICASSP), 2013 IEEE International Conference on*, pp. 6645–6649. IEEE, 2013.

Han, Song, Mao, Huizi, and Dally, William J. Deep compression: Compressing deep neural network with pruning, trained quantization and huffman coding. *CoRR, abs/1510.00149*, 2, 2015.

Han, Song, Kang, Junlong, Mao, Huizi, Hu, Yiming, Li, Xin, Li, Yubin, Xie, Dongliang, Luo, Hong, Yao, Song, Wang, Yu, et al. Ese: Efficient speech recognition engine with compressed lstm on fpga. In *FPGA 2017; NIPS 2016 EMDNN workshop*, 2016.

Hempel, Martin. Deep learning for piloted driving. In *NVIDIA GPU Tech Conference*, 2016.

Hochreiter, Sepp and Schmidhuber, Jürgen. Long short-term memory. *Neural computation*, 9(8):1735–1780, 1997.

Horowitz, M. 1.1 Computing's energy problem (and what we can do about it). In *2014 IEEE International Solid-State Circuits Conference Digest of Technical Papers (ISSCC)*, pp. 10–14, February 2014. doi: 10.1109/ISSCC.2014.6757323.

Huang, Gao, Sun, Yu, Liu, Zhuang, Sedra, Daniel, and Weinberger, Kilian. Deep networks with stochastic depth. *arXiv preprint arXiv:1603.09382*, 2016.

Iandola, Forrest N, Moskewicz, Matthew W, Ashraf, Khalid, Han, Song, Dally, William J, and Keutzer, Kurt. Squeezenet: Alexnet-level accuracy with 50x fewer parameters and¡ 1mb model size. *arXiv preprint arXiv:1602.07360*, 2016.

Laurent, Thomas and von Brecht, James. A recurrent neural network without chaos. *arXiv preprint arXiv:1612.06212*, 2016.

Leonard, R Gary and Doddington, George. Tidigits speech corpus. *Texas Instruments, Inc*, 1993.

Mikolov, Tomas, Karafiát, Martin, Burget, Lukas, Cernockỳ, Jan, and Khudanpur, Sanjeev. Recurrent neural network based language model. In *Interspeech*, volume 2, pp. 3, 2010.

Neil, Daniel and Liu, Shih-Chii. Effective sensor fusion with event-based sensors and deep network architectures. In *IEEE Int. Symposium on Circuits and Systems (ISCAS)*, 2016.

O'Connor, Peter and Welling, Max. Sigma delta quantized networks. *arXiv preprint arXiv:1611.02024*, 2016.

Ott, Joachim, Lin, Zhouhan, Zhang, Ying, Liu, Shih-Chii, and Bengio, Yoshua. Recurrent neural networks with limited numerical precision. *arXiv preprint arXiv:1608.06902*, 2016.

Rastegari, Mohammad, Ordonez, Vicente, Redmon, Joseph, and Farhadi, Ali. Xnor-net: Imagenet classification using binary convolutional neural networks. *arXiv preprint arXiv:1603.05279*, 2016.

Santana, Eder and Hotz, George. Learning a driving simulator. *arXiv preprint arXiv:1608.01230*, 2016.

Stromatias, Evangelos, Neil, Daniel, Pfeiffer, Michael, Galluppi, Francesco, Furber, Steve B, and Liu, Shih-Chii. Robustness of spiking Deep Belief Networks to noise and reduced bit precision of neuro-inspired hardware platforms. *Frontiers in Neuroscience*, 9, 2015.

Szegedy, Christian, Liu, Wei, Jia, Yangqing, Sermanet, Pierre, Reed, Scott, Anguelov, Dragomir, Erhan, Dumitru, Vanhoucke, Vincent, and Rabinovich, Andrew. Going deeper with convolutions. In *Proceedings of the IEEE Conference on Computer Vision and Pattern Recognition*, pp. 1–9, 2015.

Xu, Kelvin, Ba, Jimmy, Kiros, Ryan, Courville, Aaron, Salakhutdinov, Ruslan, Zemel, Richard, and Bengio, Yoshua. Show, attend and tell: Neural image caption generation with visual attention. *arXiv preprint arXiv:1502.03044*, 2015.

Yao, Li, Torabi, Atousa, Cho, Kyunghyun, Ballas, Nicolas, Pal, Christopher, Larochelle, Hugo, and Courville, Aaron. Describing videos by exploiting temporal structure. In *Proceedings of the IEEE International Conference on Computer Vision*, pp. 4507–4515, 2015.